

CONF-830701--12

Los Alamos National Laboratory is operated by the University of California for the United States Department of Energy under contract W-7405-ENG-36

LA-UR--83-2719

DE84 001327

TITLE: TRAC ANALYSIS OF THE CRYSTAL RIVER UNIT-3 PLANT
TRANSIENT OF FEBRUARY 26, 1980

AUTHOR(S): P. Coddington, G. J. E. Willcutt, Jr.

SUBMITTED TO: ANS Topical Meeting on "Anticipated and Abnormal Plant
Transients in Light Water Reactors," Jackson, Wyoming,
September 26-29, 1983

DISCLAIMER

This report was prepared as an account of work sponsored by an agency of the United States Government. Neither the United States Government nor any agency thereof, nor any of their employees, makes any warranty, express or implied, or assumes any legal liability or responsibility for the accuracy, completeness, or usefulness of any information, apparatus, product, or process disclosed or represents that its use would not infringe privately owned rights. Reference herein to any specific commercial product, process, or service by trade name, trademark, manufacturer, or otherwise does not necessarily constitute or imply its endorsement, recommendation, or favoring by the United States Government or any agency thereof. The views and opinions of authors expressed herein do not necessarily state or reflect those of the United States Government or any agency thereof.

MASTER

By acceptance of this article, the publisher recognizes that the U.S. Government retains a nonexclusive right to reproduce and retransmit the published form of this contribution, or to allow others to do so, for U.S. Government purposes.

DISTRIBUTION OF THIS DOCUMENT IS UNLIMITED

The Los Alamos National Laboratory requests that the publisher identify this article as work performed under the auspices of the U.S. Department of Energy.

Los Alamos Los Alamos National Laboratory
Los Alamos, New Mexico 87545

TRAC ANALYSIS OF THE CRYSTAL RIVER UNIT-3 PLANT

TRANSIENT OF FEBRUARY 26, 1980*

P. Coddington, Group Q-9**
G. J. E. Willcutt, Jr., Group Q-7

Los Alamos National Laboratory
Los Alamos, New Mexico

ABSTRACT

This paper describes the application of the TRAC-PD2 and TRAC-PF1 codes to analyze the Crystal River transient. The PD2 and PF1 analyses used the three-dimensional and one-dimensional vessel models, respectively. Both calculations predicted the plant depressurization caused by the open PORV and the subsequent repressurization caused by closing the PORV and continuing high-pressure injection flow. Also, natural circulation was calculated in loop B following reestablishment of feedwater to the loop-B steam generator. After system repressurization, the codes calculated that pressure was relieved through the safety valves, and an intermittent flow occurred in loop A because of high-pressure-injection-driven density variations.

*Work performed under the auspices of the United States Nuclear Regulatory Commission.

**On attachment from the United Kingdom Atomic Energy Authority.

I. INTRODUCTION

An automatic reactor shutdown occurred at Crystal River-3 on February 26, 1980. Interruption of a power supply to the non-nuclear instrumentation caused erroneous signals to be supplied to the integrated control system (ICS). The ICS then reduced the feedwater flow, increased the reactor power, and opened the power-operated relief valve (PORV). The resulting transient included a depressurization to 9.2 MPa followed by repressurization to the safety-relief-valve (SRV) setpoint with a large quantity of water ejected to the containment. References 1-3 describe the evolving understanding of the transient. Because much of the instrumentation was lost, only limited data is available.

This paper describes our modeling of the transient with TRAC-PD2 (Ref. 4) using a three-dimensional vessel and with TRAC-PF1 (Ref. 5) using a one-dimensional vessel. These two calculations were performed for two different task areas and are presented together in this paper to indicate differences caused by code versions, component models, and plant boundary condition assumptions. This is the first application of TRAC-PF1 with a one-dimensional vessel to a transient in an operating PWR.

II. MODEL DESCRIPTION

The PD2 and PF1 models both include two identical loops (A and B), except the pressurizer is connected to loop A. Detailed noding diagrams for the two models can be found in Ref. 6 and 7. Each loop includes a hot leg with candy cane, a steam generator, and two cold legs combined to increase calculational efficiency. Each combined cold leg includes a loop seal, a pump, and a high-pressure-injection (HPI) connection. We modeled the reactor coolant pumps using the LOFT pump characteristics in TRAC scaled with plant data. Each steam-generator secondary is attached to a main-feedwater inlet, auxiliary-feedwater inlet, and a long pipe to the steam outlet with a side connection to a safety valve. The PD2 steam-generator model did not include an aspirator model so the mixed feedwater-plus-aspirator flow was supplied as a boundary condition. The PF1 model included an aspirator model so the actual feedwater conditions were supplied at the top of the downcomer.

The PF1 vessel was modeled using one-dimensional components including the one-dimensional core component available in PF1 but not PD2. The PF1 one-dimensional representation of the vessel included two separate downcomers connected at the lower plenum

plus a cross connection at a higher elevation to model any azimuthal flows. The PD2 vessel was modeled with two azimuthal segments, two radial segments, and seven levels. The seven levels include a lower plenum, three active core levels, two levels in the upper plenum to permit the vent valves (level 6) to be above the hot- and cold-leg connections (level 5) in case of water level changes, and an upper head. Both vessel models included vent valves between the upper plenum and downcomer and connections from the upper head to each hot leg to simulate upper-head circulation.

Our PD2 analysis was based on a model developed for TMI-2 using boundary conditions from the Crystal River transient, whereas the PF1 model developed later was specifically for Crystal River. Therefore, the PD2 model used the larger TMI-2 2772-MW_{th} initial power level, and the PF1 model used 2418 MW_{th}. Also, the PD2 model used the 1979 ANS decay curve including the contribution of actinides, whereas the PF1 model used the 1979 ANS decay curve without the actinide contribution.

III. TRAC CODE DESCRIPTION

The PD2 calculation used the TRAC-PD2/MOD1 code with the following major additions: (1) a vessel vent-valve model, (2) an auxiliary-feedwater system with control based upon either a steam-generator level calculation or operator action, and (3) an improved model of the mixing of liquid and vapor between one-dimensional cells in the horizontal and vertical low-flow regimes. The PF1 calculation used the released version of the TRAC-PF1/MOD0 code, and the calculation was part of the independent assessment of PF1.

Both PD2 and PF1 allow thermal nonequilibrium between the phases. However, PD2 uses a drift-flux model to calculate the relative flow between the phases in the one-dimensional components, and PF1 independently solves the vapor and liquid momentum equations. This allows for an improved calculation of countercurrent flow. Also, it is possible to represent a one-dimensional stratified flow, which is not possible in PD2. Another major difference is PD2 calculates higher interphase condensation rates than PF1.

Finally, because the PF1 calculation used a one-dimensional core component, advantage could be taken of the one-dimensional two-step numerics in PF1 that allows the time step to exceed the material Courant limit. This was reflected in the CPU/transient time ratios which were 6.73 for PD2 and 3.21 for PF1.

IV. CALCULATION RESULTS

Table I shows the PD2 and PF1 calculated sequence of events together with plant data where available. Figures 1-3 show comparisons of PD2 and PF1 results with experimental data from Ref. 1 for system pressure, upper-plenum temperature, and loop-A mass flow rate. The non-nuclear instrumentation failure caused the PORV to open and the feedwater to both steam generators to be reduced at 1.0 s. For the calculations, the feedwater was reduced to zero over a 9-s period as was suggested in Ref. 3. The reduced feedwater flow caused an increase in primary-system pressure and a high-pressure reactor trip at 17.5 s. Coincident with the reactor trip the turbine tripped.

Steam lost through the PORV depressurized the system. Two different PORV sizes were used. The PD2 PORV was based on 110% of the design flow. The PD2 PORV size was determined on the basis of a limited sensitivity comparison of the primary system depressurization rate versus PORV size. This demonstrated that when using the best estimate feedwater reduction rate, the nominal PORV size produced too slow a primary depressurization. The PF1 PORV was based on an experimentally determined flow from Ref. 3 of 155% of the design flow. The PD2 and PF1 results bound the actual depressurization until the system begins voiding.

The reactor coolant pumps were tripped in the plant transient upon HPI initiation in line with the USNRC small-break guidelines. We specified the pump trip at the actual transient time of 224 s. The HPI flow was turned on in the calculations when the pressure decreased to 10.44 MPa as in the plant. In both calculations the pump trip was kept at 224 s even though HPI initiation occurred at different times. After the pump trip, flow was reestablished to the loop-B steam-generator secondary. The plant data, Table I, indicates that the pumps were tripped 25 s after the HPIS trip. Use of this delay would have produced pump trip times of 232 s for PF1 and 307 s for PD2.

Following pump trip, the system continued to depressurize until the liquid became saturated and voids began to form. At this point the depressurization slowed as the liquid flashed. During this period, natural-circulation flow occurred in loop B because of the secondary cooling, whereas the loop-A flow almost halted. Void formation continued, and voids collected in the loop-A candy cane and upper head. The loop-B void fraction remained low because of the continuous condensation in the steam generator. For loop A, however, there were only very small flows from the HPI entering and flow out the PORV.

As a result of the primary-coolant water flashing and of the injected HPI flow of approximately 70 kg/s, the pressurizer water level rose until the pressurizer filled at 380 s for PF1 and 420 s for PD2. Following the pressurizer filling, the primary system repressurized as the HPI flow of 70 kg/s exceeded the PORV liquid critical discharge of 25-30 kg/s. As the system repressurized, the PD2 and PF1 calculations differed because of the different condensation models. In PF1, which calculates a lower effective condensation rate, the system repressurized initially without condensing the voids. The void at the top of the loop-A candy cane then collapsed at 416 s causing a depressurization that ended at 450 s when the PORV was closed. After this a compression of the voids in the loop-B candy cane followed by their rapid collapse occurred at 520 s in both calculations. The void collapse in loop B at 520 s occurred as a result of the change from main feedwater to auxiliary feedwater in the loop-B steam-generator secondary at 510 s. This change significantly increased the cooling at the top of the steam-generator primary as the colder auxiliary feedwater entered at the top of the steam-generator secondary. The enhanced cooling increased the flow through loop B and increased the vapor condensation. This occurred because the condensation rate is dependent upon the liquid linear velocity in both codes. A temperature oscillation (Fig. 2) was seen coincident with each pressure oscillation. This resulted from an increase in loop flow as the voids in that loop collapsed. The increase in loop flow caused the stagnant hot water in the core to flow into the upper plenum. The plant pressure did not indicate a rapid void collapse. However, a change in slope of the pressure trace at 565 s indicated that all voids had condensed. The system repressurized to the SRV setpoint at 671 s for PF1 and 704 s for PD2.

Figure 2 shows the PD2, PF1, and plant transient comparison of upper-plenum temperatures. The plant data was taken from subcooling alarms up to pump trip and thermocouple data following that. The agreement is very good for the PF1 calculation. However, the plant data does not show the coolant temperature oscillations that arise both from the collapse of voids prior to 700 s and from loop-A density flow oscillations between 700 and 1800 s. Following 700 s, the PF1 rate of cooling is the same as that given by the plant data. The PD2 reduced rate of cooling and the overall higher temperature is a consequence of the higher initial power and the different decay heat assumption.

After the system repressurized to the SRV setpoint, we continued the calculations to 1800 s to determine the minimum cold-leg and downcomer temperatures. From 700 to 1800 s, the loop-B flow continued because of steam-generator cooling, and

there was no significant HPI cooling of the loop-B cold-leg fluid. However, for both calculations the loop-A flow was nearly zero for long periods of time because there was no steam-generator cooling to drive it (Fig. 3). During these quiescent periods, the HPI water entered and started spreading both ways from the injection location. When this cold high-density water reached the pipe leading down into the loop seal, the density difference produced a flow back through the loop and out the hot leg to the vessel. This reverse flow rapidly damped out as warm water from the vessel entered the cold leg and mixed with the HPI flow to remove the driving force. However, this intermittent flow prevented cold unmixed HPI water from reaching the vessel and thus the downcomer temperatures remained above 440 K (Fig. 4) even though temperatures in the cold leg near the HPI location were as low as 310 K (Fig. 5) during the quiescent periods. The intermittent flow would probably eventually stop because each surge produced a colder loop-seal temperature, and as the loop seal filled with cold water the driving potential would be removed. In the Crystal River transient, feedwater was reestablished to loop A at 2200 s, this would establish natural circulation and end the intermittent flow.

We have two concerns about this intermittent reverse flow process. First, it may be a characteristic of a one-dimensional model that perhaps would be eliminated by a multidimensional loop-seal model that permitted cold water to flow down one side of the pipe while warmer water moved up countercurrent to it. Second, if it does occur, a model that included both cold legs in each loop might show a flow from the vessel into one cold leg and back out the other cold leg to the vessel. More downcomer cooling could result as the cold HPI from one of the cold legs flows into the downcomer.

V. CONCLUSIONS AND RECOMMENDATIONS

Two TRAC simulations of the Crystal River transient were performed. The first used TRAC-PD2 with a three-dimensional vessel, and the second used TRAC-PF1 with a one-dimensional vessel.

PD2 and PF1 calculated the system depressurization well, and the differences reflect the different PORV areas used. Following the reactor-coolant-pump trip, feedwater was reestablished to loop B, resulting in natural circulation in this loop. This was calculated well by both codes. The system repressurization following the PORV closure, was also calculated well by the codes. However, because of the nature of the condensation

models, the codes calculated two condensation-induced pressure oscillations during the repressurization.

PF1 calculated the overall cooling well, but PD2 indicated that the core power was too large based on a different plant model and decay-heat assumption.

After the system repressurized, there was no established flow in loop A because there was no steam-generator cooling to drive it. This resulted in the HPI flow collecting in the cold leg, and because the HPI injection point is close to the pump, the cold water flowed back through the pump to the loop seal producing gravity-driven reverse flows through loop A. This therefore reduced the HPI water flow to the downcomer, and downcomer temperatures never went below 440 K for either calculation.

We recommend that tests be conducted in large pipes to determine if this reverse flow is a potential phenomenon of concern or is just an artifact of one-dimensional models.

REFERENCES

1. "Transient Assessment Report--Reactor Trip at Crystal River-3 Nuclear Station on February 26, 1980 (Preliminary)," Babcock & Wilcox report 07-08-02, Rev. 02 (March 9, 1980).
2. "Analysis and Evaluation of Crystal River--Unit 3 Incident," Nuclear Safety Analysis Center report NSAC-3 (March 1980).
3. W. Brown, G. Caldwell, B. Chexal, and W. Layman, "Thermohydraulic Analysis of Crystal River Unit-3 Incident," Nuclear Safety Analysis Center report NSAC-15 (June 1981).
4. "TRAC-PD2 An Advanced Best-Estimate Computer Program for Pressurized Water Reactor Loss-of-Coolant Accident Analysis," Los Alamos National Laboratory report LA-8709-MS, NUREG/CR-2054 (April 1981).
5. "TRAC-PF1 An Advanced Best-Estimate Computer Program for Pressurized Water Reactor Analysis," Los Alamos National Laboratory report to be published.
6. G. J. E. Willcutt, Jr. "TRAC-PD2 Calculations of the Crystal-River-3 Transient of February 26, 1980 Using Revised Assumptions", Los Alamos National Laboratory report LA-UR-83-1078 (April 1983).
7. P. Coddington, "TRAC-PF1 One-Dimensional Analysis of the Crystal River Unit 3 Plant Transient of February 26, 1980", Los Alamos National Laboratory report to be published.

TABLE I
TRANSIENT EVENT SEQUENCE
TIME(s)

| TRAC-PF1 | TRAC-PD2 | Plant ¹ <u>Data</u> | <u>Event</u> |
|--------------------------------------|--------------------------------------|---|---|
| 0 | 0 | 0 | Non-nuclear instrumentation failure. |
| 1 | 1 | 1 | PORV open. Feedwater begins to ramp down. |
| 10 | 10 | | Feedwater off. |
| 17.6 | 17.5 | 10-25 ¹ 25.5 ² | Reactor trip. |
| 207 | 282 | 201 ³ 235 ⁴ | HPIS trip. Pressure falls below 10.44 MPa (1500 psig). |
| 224 ⁵ 232 ⁵ | 224 ⁵ 307 ⁵ | 224-227 224 ² | Reactor coolant pump trip. |
| 224-229 | 225-229 | 224-227 224 ² | Feedwater reestablished to loop B. |
| 245 | 260 | | Initial void formation. |
| 320 | 333 | | Loop A flow stalls on candy cane high void fraction. |
| 380 | 420 | | Pressurizer liquid solid. |
| 450 | 450 | 280-520 450 ² | Closure of PORV block valve. |
| 510 | 510 | 510 ² | Main feedwater turned off. Auxiliary feedwater turned on to loop B. |
| 671 | 704 | 591 ⁶ 595-610 ⁷ ~620 ⁸ | SRV open first time (system repressurized). |

TABLE I (continued)

1. Plant data taken from Ref. 1.
2. Data taken from Ref. 3.
3. Times taken from Ref. 1, Event Synopsis.
4. Times taken from Ref. 1, Fig. III-3.
5. RCS pump trip; on basis of HPIS trip + 25 s delay as indicated by plant data.
6. Reference 1, Event Synopsis
Reactor Coolant System pressure 16.38 MPa (2361 psig).
7. Reference 1, Event Synopsis SRV opened.
8. Reference 1, Fig. III-3 and III-4.

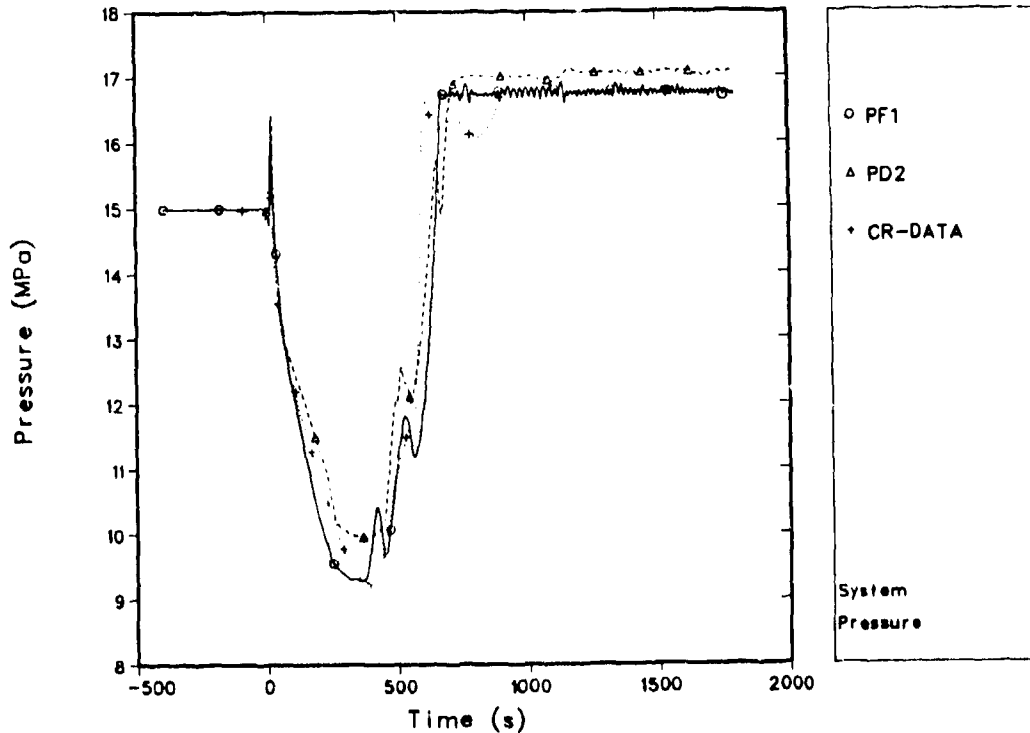


Fig. 1.
Primary coolant system pressure.

-10-

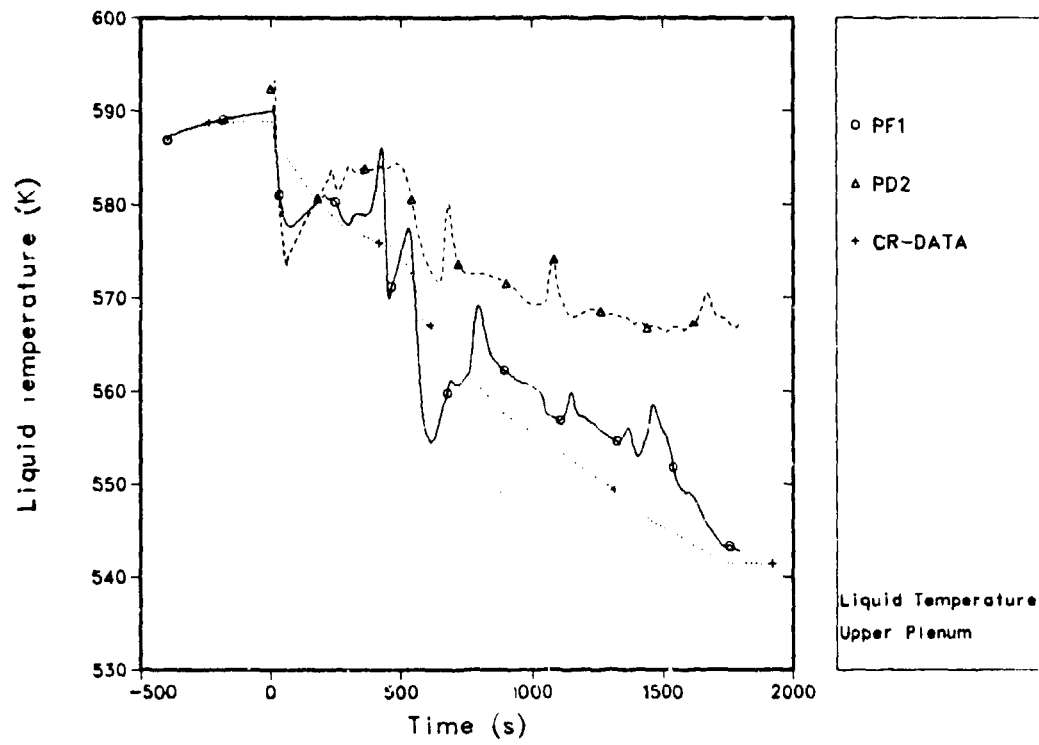


Fig. 2.
Upper-plenum liquid temperature.

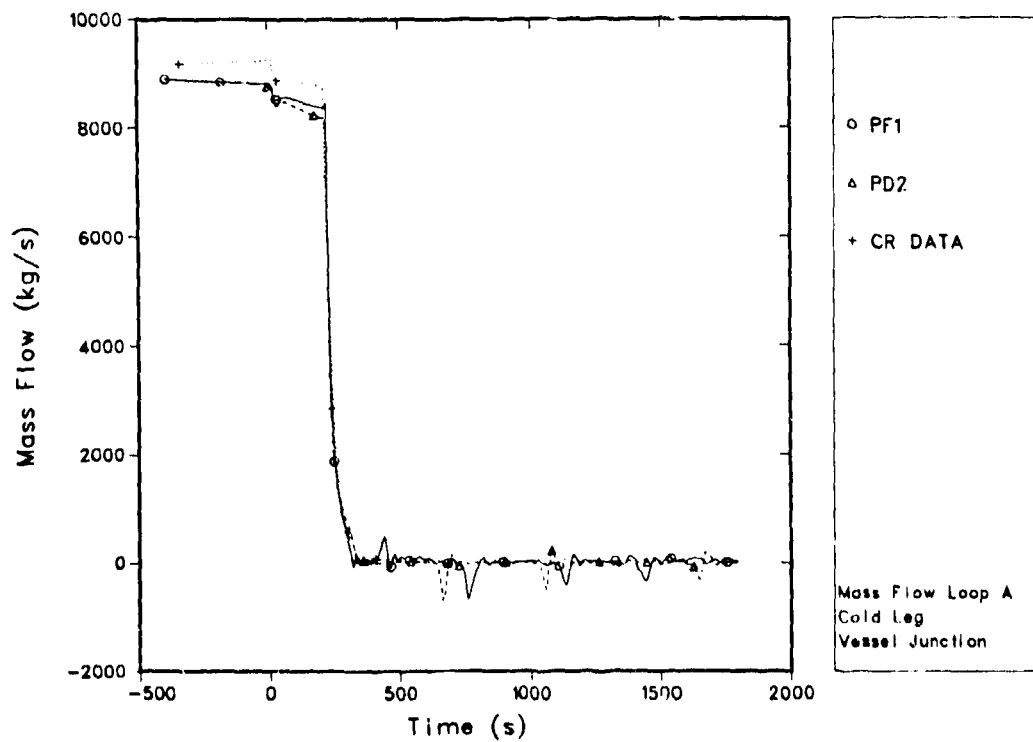


Fig. 3.
Loop-A mass flow

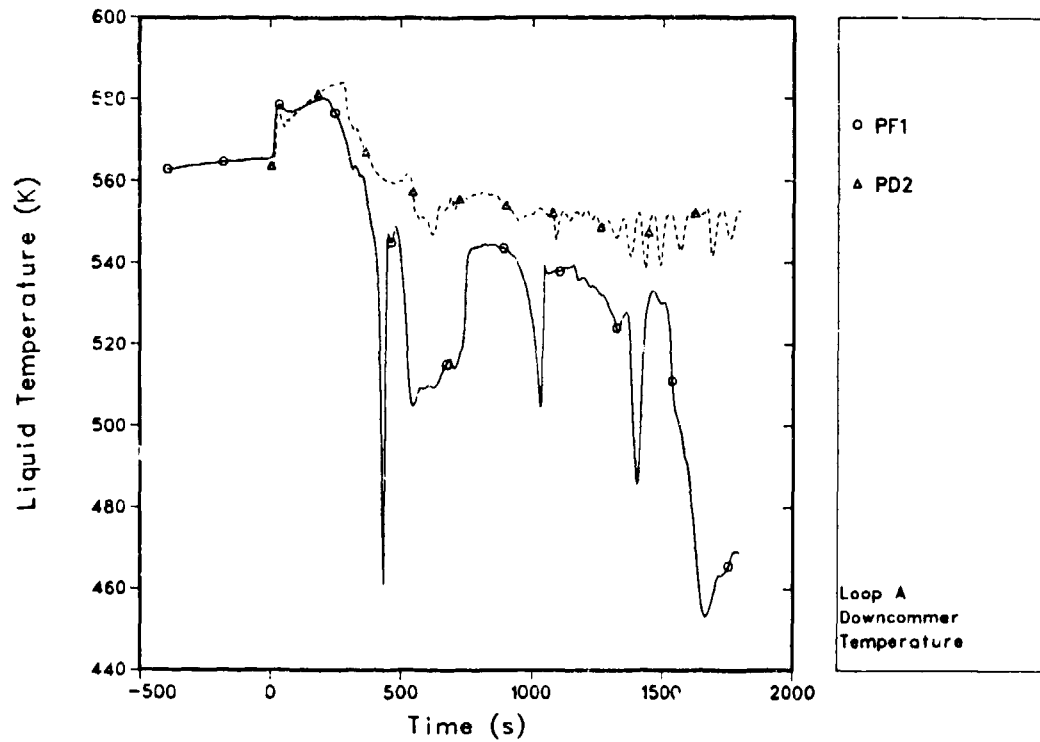


Fig. 4.
Loop-A downcomer liquid temperature.

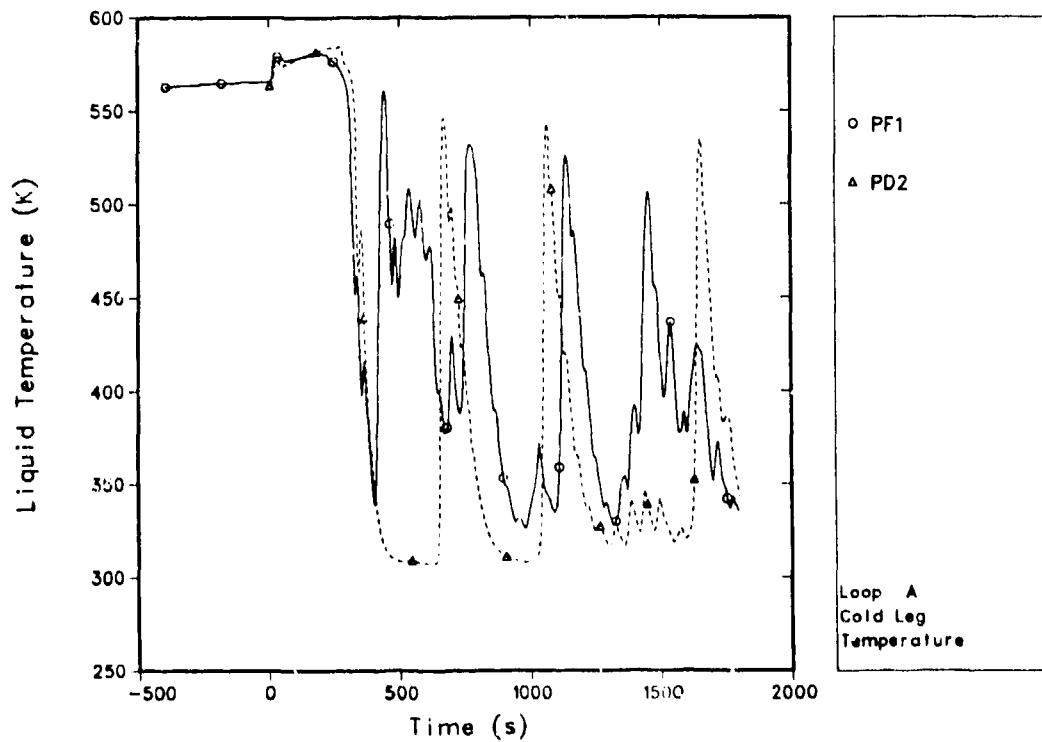


Fig. 5.
Loop-A cold-leg liquid temperature.